Journal of Coordination Chemistry

ISSN: 0095-8972 (Print) 1029-0389 (Online) Journal homepage: http://www.tandfonline.com/loi/gcoo20

Synthesis, structures and magnetic properties of two isomeric coordination polymers constructed from pamoic acid and 1,2-di(4-pyridyl)ethane

Xianzhong Bu, Zongwu Wei & Shaofeng Ren

To cite this article: Xianzhong Bu, Zongwu Wei & Shaofeng Ren (2015) Synthesis, structures and magnetic properties of two isomeric coordination polymers constructed from pamoic acid and 1,2-di(4-pyridyl)ethane, Journal of Coordination Chemistry, 68:3, 471-478, DOI: 10.1080/00958972.2014.998209

To link to this article: http://dx.doi.org/10.1080/00958972.2014.998209

Accepted author version posted online: 15 Dec 2014.
Published online: 02 Jan 2015.

Journal of Coordination Chemistry, 2015
Vol. 68, No. 3, 471–478, http://dx.doi.org/10.1080/00958972.2014.998209

Synthesis, structures and magnetic properties of two isomeric coordination polymers constructed from pamoic acid and 1,2-di(4-pyridyl)ethane

XIANZHONG BU†, ZONGWU WEI*‡ and SHAOFENG REN§

†College of Materials and Mineral Resources, Xi'an University of Architecture and Technology, Xi'an, China
‡College of Resources and Metallurgy, Guangxi University, Nanning, China
§Southwest Energy and Mineral Resources Corporation Co., Ltd., Guiyang, China

(*Received 14 May 2014; accepted 10 November 2014*)

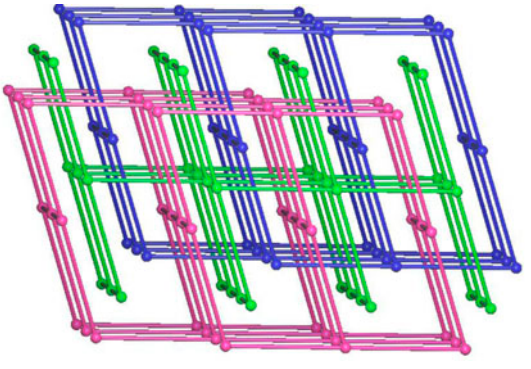

Presented here are two isomeric compounds constructed from pamoic acid and 1,2-di(4-pyridyl)ethane, which are 3-D frameworks with threefold interpenetrated cds topology.

Two isostructural compounds, $[Co(pam)(bpe)(H_2O)_2]_n$ (**1**) and $[Mn(pam)(bpe)(H_2O)_2]_n$ (**2**) (H_2pam = pamoic acid, bpe = 1,2-di(4-pyridyl)ethane), have been solvothermally synthesized and characterized by elemental analyses, IR, and powder X-ray diffraction. Single-crystal X-ray analysis reveals that **1** and **2** are isostructural and feature a threefold interpenetrated **cds** topological framework. Magnetic investigations reveal that both **1** and **2** exhibit antiferromagnetic properties.

Keywords: Pamoic acid; Isostructure; Solvothermal synthesis; Antiferromagnetic property

1. Introduction

Metal–organic frameworks have attracted much interest for esthetic architectures and potential applications as functional materials in luminescence, nonlinear optics, catalysis,

*Corresponding author. Email: zongwu_wei66@163.com

gas storage and separation, magnetism, etc. [1–5]. However, the rational design and synthesis of MOFs remains an elusive goal in crystal engineering. For self-assembly processes of MOFs, there are two important factors for design and synthesis of target structures with functional properties: one is the judicious selection of metal centers and organic ligands, and the other is the choice of the synthetic strategy. Among various ligands, polycarboxylated ligands have proven to be good candidates for the construction of MOFs owing to the variety of coordination modes and strong bonding abilities to metal ions [6–9]. In addition, N-containing ligands are used to tune the dimensionality or interpenetration of the MOFs [10–12]. Mixed ligand self-assembly is one of the most effective methods to synthesize new compounds with predictable structures [13]. By employing this strategy, a great number of MOFs have been synthesized [14–17]. Pamoic acid (H_2pam) contains six potential coordination sites, which can display various coordination modes to metal ions. There also exists a flexible $–CH_2–$ group, which can enable the acid to adopt suitable configurations according to geometric requirements of different metal ions during the self-assembly process. 1,2-Di(4-pyridyl)ethane (bpe), as a flexible bridging ligand, is often used as an auxiliary ligand to construct higher dimensional MOFs. For example, Wang and co-workers not only reported a series of 4-connected entangled MOFs constructed from pamoic acid and pyridine-containing ligands, but also reported three new temperature-dependent Zn(II) supramolecular isomers based on pamoic acid and imidazole-containing flexible ligands [18, 19]. Lv and co-workers also reported a 2-D→3-D polythreaded compound and a 2-D 4-connected tetragonal plane compound, which are also constructed from pamoic acid and N-containing auxiliary ligands [20]. Based on the above considerations, we adopt a mixed ligand self-assembly strategy using H_2pam and bpe as ligands, obtaining two isomeric compounds, $[Co_2(pam)(bpe)(H_2O)_2]_n$ (**1**) and $[Mn_2(pam)(bpe)(H_2O)_2]_n$ (**2**) (H_2pam = pamoic acid, bpe = 1,2-di(4-pyridyl)ethane). Herein, we report the syntheses, structures, and magnetic properties.

2. Experimental

2.1. *Materials and instrumentation*

All reagents and solvents were commercially available and used without purification. IR spectra were measured with a PECO (USA) SpectrumOne spectrophotometer as KBr pellets were from 4000 to 400 cm^{-1}. Elemental analyses (C, H and N) were determined with an elemental Vario EL III analyzer. Powder X-ray diffraction (PXRD) analyses were recorded on a PANalytical X'Pert Pro powder diffractometer with Cu/Kα radiation (λ = 1.54056 Å) with a step size of 0.05°. The polycrystalline magnetic susceptibility data were collected on a Quantum Design MPMS (SQUID)-XL magnetometer from 2 to 300 K.

2.2. *Synthesis of $[Co_2(pam)(bpe)(H_2O)_2]_n$ (1)*

A mixture of $CoCl_2 \cdot 6H_2O$ (0.1 mM, 0.024 g), H_2pam (0.1 mM, 0.038 g), bpe (0.1 mM, 0.018 g), DMA (2 mL), and H_2O (2 mL) were sealed into a teflon-lined stainless-steel reactor under autogenous pressure at 130 °C for 3 days and then cooled to room temperature slowly. The obtained clear solution was evaporated for one week and purple block crystals of **1** were obtained in 45% yield based on Co(II). Elemental analyses: Anal. Calcd for $C_{35}H_{30}CoN_2O_8$: C, 63.10%; H, 4.51%; N, 4.21%. Found: C, 63.15%; H, 4.48%; N, 4.23%.

Selected IR peaks (cm^{-1}): 3452(s), 2257(s), 1640(m), 1612(s), 1576(s), 1507(m), 1460(s), 1343(m), 1230(m), 827(s), 753(m).

2.3. *Synthesis of $[Mn_2(pam)(bpe)(H_2O)_2]_n$ (2)*

Synthesis of **2** was similar to that of **1**, but with $MnCl_2{\cdot}4H_2O$ (0.1 mM, 0.19 g) in place of $CoCl_2{\cdot}6H_2O$. Pink crystals of **2** were obtained in 43% yield based on Mn(II). Elemental analyses: Anal. Calcd for $C_{35}H_{30}MnN_2O_8$: C, 63.49%; H, 4.53%; N, 4.23%. Found: C, 63.43%; H, 4.51%; N, 4.20%. Selected IR peaks (cm^{-1}): 3453(s), 2256(s), 1640(m), 1612(s), 1575(s), 1507(m), 1461(s), 1342(m), 1234(m), 822(s), 751(m).

2.4. *X-ray crystallography*

Suitable single crystals of **1** and **2** were carefully selected under an optical microscope and glued to thin glass fibers. Structural measurements were performed with a computer-controlled Bruker Smart Apex-II CCD diffractometer with graphite-monochromated Mo–Kα radiation (λ = 0.71073 Å) at T = 293(2) K. Absorption corrections were made using SADABS [21]. The structures were solved using direct methods and refined by full-matrix least-squares on F^2 using the SHELXL-97 program package [22]. All nonhydrogen atoms were refined anisotropically and hydrogens were placed geometrically and refined using the riding model. Crystal data as well as details of data collection and refinements of **1** and **2** are summarized in table 1; selected bond lengths and angles are given in table 2.

3. Results and discussion

3.1. *Description of crystal structure*

Compounds **1** and **2** are isostructural; herein, only the structure of **1** as a representative is described in detail. Single crystal X-ray structural analysis reveals that **1** crystallizes in the

Table 1. Crystal data and structure refinements for **1** and **2**.

	1	**2**
Formula	$C_{35}H_{30}CoN_2O_8$	$C_{35}H_{30}MnN_2O_8$
Fw	665.54	661.55
Crystal system	Monoclinic	Monoclinic
Space group	*P 2₁/c*	*P 2₁/c*
a (Å)	12.839(15)	14.1005(9)
b (Å)	18.670(18)	17.8578(11)
c (Å)	14.557(17)	14.0921(8)
β (°)	96.72(3)	96.021(3)
Volume ($Å^3$)	3465(7)	3528.9(4)
Z	4	4
Density (calculated)	1.276	1.245
Abs. coeff. (mm^{-1})	0.546	0.424
Total reflections	20,033	20,209
Unique reflections	6071	6208
Goodness-of-fit on F^2	1.046	1.004
Final *R* indices [$I > 2\sigma(I^2)$]	R = 0.0841, wR_2 = 0.2390	R = 0.0479, wR_2 = 0.1243
R (all data)	R = 0.1142, wR_2 = 0.2607	R = 0.0648, wR_2 = 0.1352

Table 2. Selected bond lengths (Å) and angles (°) for **1** and **2**.

1			
Co(1)–O(2 W)	2.026(5)	Co(1)–O(2 W)^{a}	2.026(5)
Co(1)–O(5)^{a}	2.126(4)	Co(1)–O(5)	2.126(4)
Co(1)–N(2)^{b}	2.202(5)	Co(1)–N(2)^{c}	2.202(5)
Co(2)–O(1)	2.057(4)	Co(2)–O(1)^{d}	2.057(4)
Co(2)–O(1 W)	2.179(4)	Co(2)–O(1 W)^{d}	2.179(4)
Co(2)–N(1)	2.227(4)	Co(2)–N(1)^{d}	2.227(4)
O(2 W)–Co(1)–O(2 W)^{a}	180.0(3)	O(2 W)–Co(1)–O(5)^{a}	89.20(19)
O(2 W)^{a}–Co(1)–O(5)^{a}	90.80(19	O(2 W)–Co(1)–O(5)	90.80(19)
O(2 W)^{a}–Co(1)–O(5)	89.20(19)	O(5)^{a}–Co(1)–O(5)	180.00(9)
O(2 W)–Co(1)–N(2)^{b}	92.2(2)	O(2 W)^{a}–Co(1)–N(2)^{b}	87.8(2)
O(5)^{a}–Co(1)–N(2)^{b}	88.97(17)	O(5)–Co(1)–N(2)^{b}	91.03(17)
O(2 W)–Co(1)–N(2)^{c}	87.8(2)	O(2 W)^{a}–Co(1)–N(2)^{c}	92.2(2)
O(5)^{a}–Co(1)–N(2)^{c}	91.03(17)	O(5)–Co(1)–N(2)^{c}	88.97(17)
N(2)^{b}–Co(1)–N(2)^{c}	180.000(1)	O(1)–Co(2)–O(1)^{d}	180.0(2)
O(1)–Co(2)–O(1 W)	87.73(16)	O(1)^{d}–Co(2)–O(1 W)	92.27(16)
O(1)–Co(2)–O(1 W)^{d}	92.27(16)	O(1)^{d}–Co(2)–O(1 W)^{d}	87.73(16)
O(1 W)–Co(2)–O(1 W)^{d}	180.0(2)	O(1)–Co(2)–N(1)	93.30(17)
O(1)^{d}–Co(2)–N(1)	86.70(17)	O(1 W)–Co(2)–N(1)	91.09(17
O(1 W)#4–Co(2)–N(1)	88.91(17)	O(1)–Co(2)–N(1)^{d}	86.70(17)
O(1)^{d}–Co(2)–N(1)^{d}	93.30(17)	O(1 W)–Co(2)–N(1)^{d}	88.91(17)
O(1 W)^{d}–Co(2)–N(1)^{d}	91.09(17)	N(1)–Co(2)–N(1)^{d}	180.0(3)
2			
Mn(1)–O(4)^{a}	2.1099(18)	Mn(1)–O(4)	2.1100(18)
Mn(1)–O(1 W)^{a}	2.2239(19)	Mn(1)–O(1 W)	2.2239(19)
Mn(1)–N(2)^{b}	2.319(2)	Mn(1)–N(2)^{c}	2.319(2)
Mn(2)–O(1)	2.1549(18)	Mn(2)–O(1)^{d}	2.1549(18)
Mn(2)–O(2 W)	2.193(2)	Mn(2)–O(2 W)^{d}	2.193(2)
Mn(2)–N(1)^{d}	2.280(2)	Mn(2)–N(1)	2.280(2)
O(4)^{a}–Mn(1)–O(4)	180.000(1)	O(4)^{a}–Mn(1)–O(1 W)^{a}	90.61(8)
O(4)–Mn(1)–O(1 W)^{a}	89.39(8)	O(4)^{a}–Mn(1)–O(1 W)	89.39(8)
O(4)–Mn(1)–O(1 W)	90.61(8)	O(1 W)^{a}–Mn(1)–O(1 W)	180.00(13)
O(4)^{a}–Mn(1)–N(2)^{b}	85.20(8)	O(4)–Mn(1)–N(2)^{b}	94.80(8)
O(1 W)^{a}–Mn(1)–N(2)^{b}	92.77(8)	O(1 W)–Mn(1)–N(2)^{b}	87.23(8)
O(4)^{a}–Mn(1)–N(2)^{c}	94.80(8)	O(4)–Mn(1)–N(2)^{c}	85.20(8)
O(1 W)^{a}–Mn(1)–N(2)^{c}	87.23(8)	O(1 W)–Mn(1)–N(2)^{c}	92.77(8)
N(2)^{b}–Mn(1)–N(2)^{c}	180.0	O(1)–Mn(2)–O(1)^{d}	180.000(1)
O(1)–Mn(2)–O(2 W)	87.57(8)	O(1)^{d}–Mn(2)–O(2 W)	92.43(8)
O(1)–Mn(2)–O(2 W)^{d}	92.43(8)	O(1)^{d}–Mn(2)–O(2 W)^{d}	87.57(8)
O(2 W)–Mn(2)–O(2 W)^{d}	180.0	O(1)–Mn(2)–N(1)^{d}	89.24(8)
O(1)^{d}–Mn(2)–N(1)^{d}	90.76(8)	O(2 W)–Mn(2)–N(1)^{d}	90.51(8)
O(2 W)^{d}–Mn(2)–N(1)^{d}	89.49(8)	O(1)–Mn(2)–N(1)	90.76(8)
O(1)^{d}–Mn(2)–N(1)	89.24(8)	O(2 W)–Mn(2)–N(1)	89.49(8)
O(2 W)^{d}–Mn(2)–N(1)	90.51(8)	N(1)^{d}–Mn(2)–N(1)	180.00(12)

Notes: Symmetry codes: Compound **1** (a) $-x+2, -y, -z+2$; (b) $x, -y+1/2, z+3/2$; (c) $-x+2, y-1/2, -z+1/2$; (d) $-x+1, -y, -z$. Compound **2** (a): $-x+2, -y, -z+1$; (b) $x, -y+1/2, z+3/2$; (c) $-x+2, y-1/2, -z-1/2$; (d) $-x+1, -y, -z-1$.

monoclinic *P 2₁/c* space group and features a threefold interpenetrated 3-D framework. The asymmetric unit of **1** contains two crystallographically independent Co(II) ions, one pam, one bpe, and two coordinated waters. As shown in figure 1, both Co_1 and Co_2 are six-coordinate with octahedral coordination geometries with two carboxylate oxygens from two different pam ligands and two nitrogens from two different bpe ligands occupying the equatorial plane, and two coordinated water molecules in the axial sites. The Co(II)–O and Co(II)–N distances are 2.026(5)–2.179(4) Å and 2.202(5)–2.227(4) Å, respectively, which are all in the expected range according to previously reported literature. In **1**, each pam bridges two Co(II) ions with its two carboxylates in monodentate mode. Under the synergistic effect

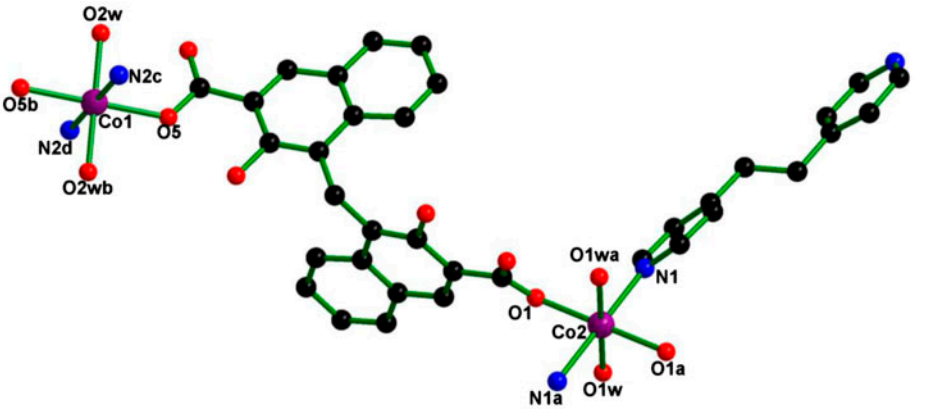

Figure 1. View of the asymmetric unit of **1**. Symmetry codes: (a) 1 – *x*, –*y*, –*z*; (b) 2 – *x*, –*y*, 2 – z; (c) 2 – *x*, –0.5 + *y*, 0.5 – *z*; and (d) *x*, 0.5 – *y*, 1.5 + *z*.

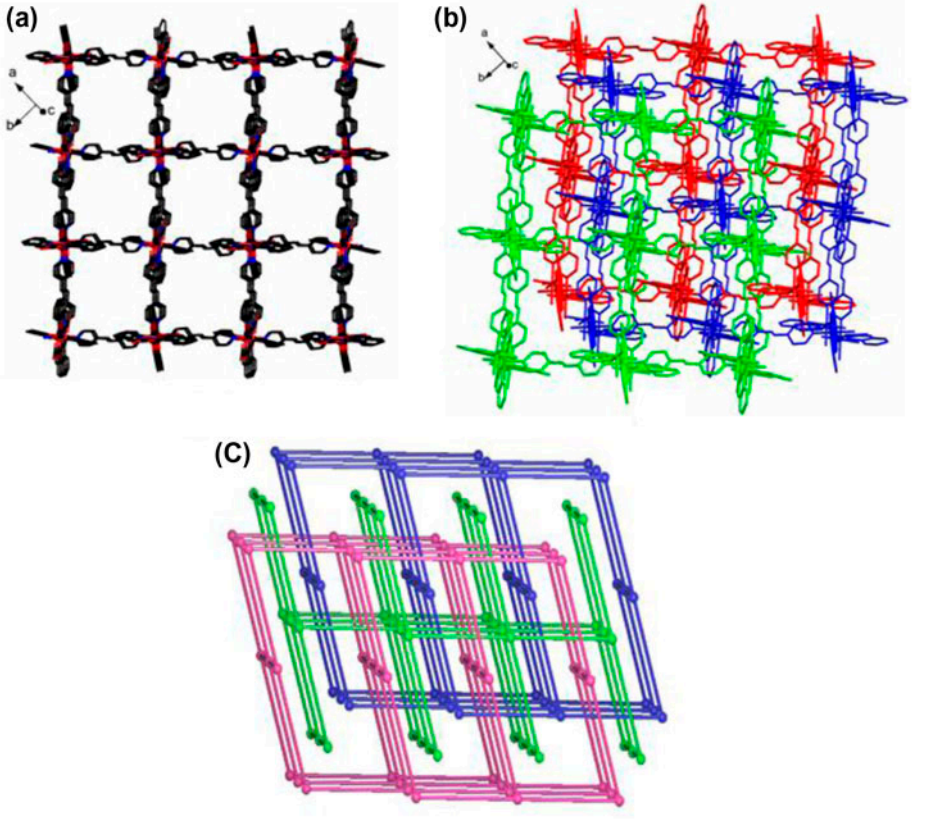

Figure 2. (a) View of the 3-D framework of **1**. (b) Threefold interpenetrated 3-D framework of **1**. (c) Schematic representation of threefold interpenetrated **cds** topological network.

of bpe and pam, all Co(II) ions are linked together, affording a 3-D framework [figure 2(a)]. Large 1-D channels exist along the crystallographic *c*-axis. The channels accommodate two identical networks. Thus, the final framework of **1** is threefold interpenetrated [figure 2(b)]. By viewing the Co(II) ions as 4-connected nodes, bpe and pam ligands as linkers, the whole framework can be reduced into a threefold interpenetrated **cds** topological network with the Schläfli symbol of $\{6^5.8\}$ [figure 2(c)] [23]. Compared with the ideal **cds** network, the **cds** network presented here is distorted, because two different linkers (pam and bpe) make the 4-connected nodes distorted from the square planarity [24].

3.2. *PXRD patterns and thermal analysis*

The experimental PXRD patterns match well with the simulated ones based on the single-crystal X-ray diffraction data, indicating that the bulk samples of **1** and **2** are in pure phase [figure 3(a) and (b)]. The thermal analyses reveal that **1** and **2** have similar thermal stability [figure 3(c) and (d)]. For **1**, the first weight loss occurs at 137–160 °C, corresponding to release of coordinated water (obsd: 5.46%, calcd: 5.41%). Then it is stable at 340 °C. After that dramatic weight loss begins owing to the decomposition of the organic ligand. For **2**, departure of the coordinated water (obsd: 5.38%, calcd: 5.44%) occurs at 124–153 °C. Then it is stable at 300 °C. Upon heating above 300 °C, the framework of **2** begins to collapse, owing to decomposition of the organic ligands.

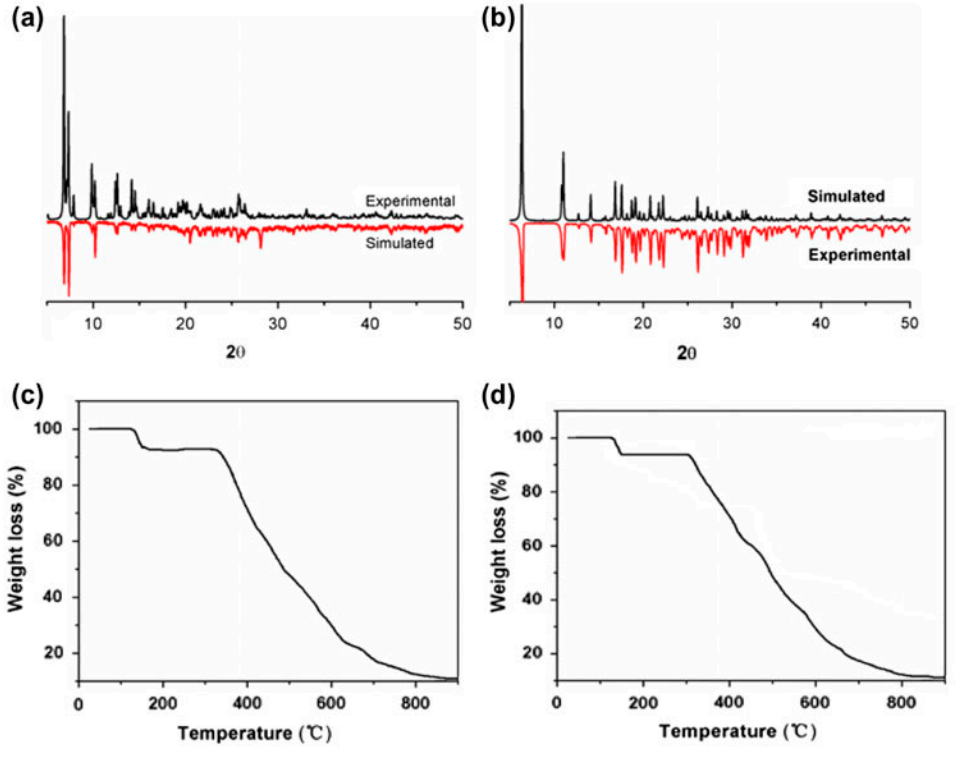

Figure 3. PXRD patterns (a) for **1** and (b) for **2**. TGA curves (c) for **1** and (d) for **2**.

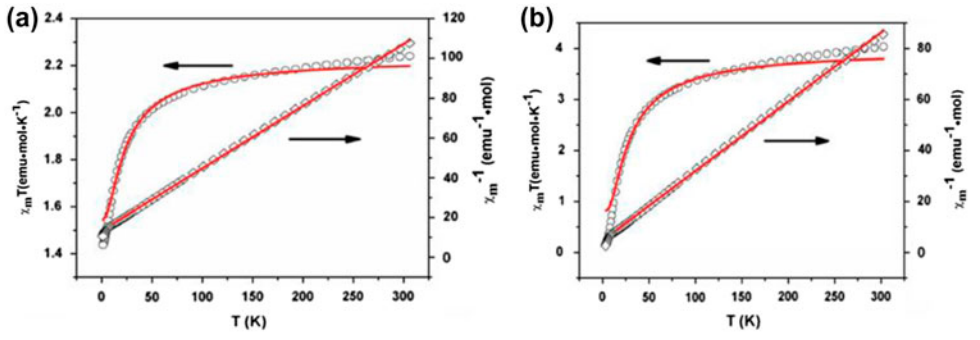

Figure 4. Temperature dependence of $\chi_m T$ and $\chi_m{}^{-1}$ under applied field of 1000 Oe (a) for **1** and (b) for **2**.

3.3. *Magnetic properties of 1 and 2*

The temperature-dependent magnetic properties of **1** and **2** in the form of $\chi_m T$ *vs.* T are shown in figure 4. For **1**, the $\chi_m T$ value of 2.23 emu M^{-1} K at 300 K is much larger than the value of one magnetically insulated high-spin Co(II) ion ($S = 3/2$, $g = 2.0$) owing to the strong spin–orbital coupling interactions for Co(II) ions. As temperature decreases, the value of $\chi_m T$ slowly decreases to a minimum of 1.43 emu M^{-1} K at 2 K. The inverse magnetic susceptibility as a function of temperature is linear above 12 K, obeying the Curie–Weiss law $\chi_m = C/(T - \theta)$ with $C = 3.23$ emu M^{-1} K and $\theta = -1.25$ K. For **2**, the $\chi_m T$ value at 300 K is 4.08 emu M^{-1} K, lower than the spin-only value of 4.375 emu M^{-1} K expected for one magnetically isolated Mn(II) ion ($S = 5/2$, $g = 2.0$). The $\chi_m T$ value steadily decreases with decreasing temperature to reach a minimum value of 0.126 emu M^{-1} K at 2 K. Above 13 K, the data of magnetic susceptibility can be fitted to the Curie–Weiss law $\chi_m = C/(T - \theta)$, giving $C = 12.30$ emu M^{-1} K and $\theta = -14.29$ K. These negative Weiss constants ($\theta = -1.25$ K for **1** and $\theta = -14.29$ K for **2**) indicate that there exists weak antiferromagnetic exchange between Co(II) ions and Mn(II) ions [25, 26].

4. Conclusion

Two isomorphic compounds, $[Co_2(pam)(bpe)(H_2O)_2]_n$ (**1**) and $[Mn_2(pam)(bpe)(H_2O)_2]_n$ (**2**), based on pam and bpe ligands have been synthesized under solvothermal conditions. The two compounds feature a threefold interpenetrated 3-D framework with 4-connected **cds** topology. Magnetic investigations reveal that both **1** and **2** exhibit antiferromagnetic behavior.

Supplementary material

CCDC Nos. 1014009–1014010 contain the supplementary crystallographic data for this article. These data can be obtained free of charge at www.ccdc.cam.ac.uk/conts/retrieving.html [or from the Cambridge Crystallographic Data Center, 12 Union Road, Cambridge CB2 1EZ, UK; Fax: (internat.) +44 1223/336 033; Email: deposit@ccdc.cam.ac.uk].

Funding

This work was supported by Guangxi Science and Technology Project [grant number 1355002-1], the Natural Science Basic Research Plan in Shaanxi Province of China [grant number 2013JM7024], and China Postdoctoral Science Foundation funded project [grant number 2013M541935].

References

[1] M. O'Keeffe. *Chem. Soc. Rev.*, **38**, 1215 (2009).
[2] S.M. Fang, Q. Zhang, M. Hu, X.G. Yang, L.M. Zhou, M. Du, C.S. Liu. *Cryst. Growth Des.*, **10**, 4773 (2010).
[3] M. Fujita, M. Tominaga, K. Suzuki, M. Kawano, T. Kusukawa. *Angew. Chem. Int. Ed.*, **43**, 5621 (2004).
[4] X.M. Shi, M.X. Li, X. He, H.J. Liu, M. Shao. *Polyhedron*, **29**, 2075 (2010).
[5] S.N. Wang, R.R. Yun, Y.Q. Peng, Q.F. Zhang, J. Lu, J.M. Dou, J.F. Bai, D.C. Li, D.Q. Wang. *Cryst. Growth Des.*, **12**, 79 (2012).
[6] X. Zhang, Y.Y. Huang, M.J. Zhang, J. Zhang, Y.G. Yao. *Cryst. Growth Des.*, **12**, 3231 (2012).
[7] F. Luo, Y.T. Yang, Y.X. Che, J.M. Zheng. *CrystEngComm*, **12**, 3231 (2008).
[8] Z.B. Han, G.X. Zhang. *CrystEngComm*, **12**, 348 (2010).
[9] S.N. Wang, Y.Q. Peng, X.L. Wei, Q.F. Zhang, D.Q. Wang, J.M. Dou, D.C. Li, J.F. Bai. *CrystEngComm*, **13**, 5313 (2011).
[10] Y.X. Tan, Y.P. He, J. Zhang. *Inorg. Chem.*, **51**, 9649 (2012).
[11] J.D. Lin, J.W. Cheng, S.W. Du. *Cryst. Growth Des.*, 8, 3345 (2008).
[12] Y.P. He, Y.X. Tan, J. Zhang. *Chem. Commun.*, **49**, 11323 (2013).
[13] Y.X. Chen, S.J. Liu, Y.W. Li, G.R. Li, K.H. He, Z. Chang, X.H. Bu. *CrystEngComm*, **15**, 1613 (2013).
[14] Z.X. Li, X. Chu, G.H. Cui, Y. Liu, L. Li, G.L. Xue. *CrystEngComm*, **13**, 1984 (2011).
[15] F. Guo, F. Wang, H. Yang, X.L. Zhang. *Inorg. Chem.*, **51**, 9677 (2012).
[16] F. Guo, B.Y. Zhu, M.L. Liu, X.L. Zhang, J. Zhang, J.P. Zhao. *CrystEngComm*, **15**, 6191 (2013).
[17] G.B. Yang, Z.H. Sun. *Inorg. Chem.*, **29**, 94 (2013).
[18] S.N. Wang, R.R. Yun, Y.Q. Peng, Q.F. Zhang, J. Lu, J.M. Dou, J.F. Bai, D.C. Li, D.Q. Wang. *Cryst. Growth Des.*, **12**, 79 (2012).
[19] S.N. Wang, Y.Q. Peng, X.L. Wei, Q.F. Zhang, D.Q. Wang, J.M. Dou, D.C. Li, J.F. Bai. *CrystEngComm*, **13**, 5313 (2011).
[20] C.W. Lv, J. Li, Z. Hou, M.K. Li. *J. Inorg. Organomet. Polym.*, **24**, 485 (2014).
[21] G.M. Sheldrick. *SADABS*, University of Göttingen, Göttingen, Germany (1996).
[22] G.M. Sheldrick. *SHELXS 97, Program for Solution of Crystal Structures*, University of Göttingen, Göttingen, Germany (1997).
[23] H. Gao, X.H. Lou, Q.T. Li, W.J. Du, C. Xu. *J. Inorg. Organomet. Polym.*, **24**, 485 (2014).
[24] J. Zhang, Y.B. Chen, Z.J. Li, Y.Y. Qin, Y.G. Yao. *Inorg. Chem. Commun.*, **9**, 449 (2006).
[25] X.Y. Zhang, Z.Y. Liu, Y.F. Xia, Y.Y. Zhang, E.C. Yang, X.J. Zhao. *J. Coord. Chem.*, **66**, 4399 (2013).
[26] X.Q. Zhao, Y.C. Li. *J. Coord. Chem.*, **66**, 931 (2013).